

# Exploring Audio Cues for Enhanced Test-Time Video Model Adaptation

Runhao Zeng, Qi Deng, Ronghao Zhang, Shuaicheng Niu, Jian Chen, Xiping Hu, Victor C. M. Leung

**Abstract**—Test-time adaptation (TTA) aims to boost the generalization capability of a trained model by conducting self-/unsupervised learning during the testing phase. While most existing TTA methods for video primarily utilize visual supervisory signals, they often overlook the potential contribution of inherent audio data. To address this gap, we propose a novel approach that incorporates audio information into video TTA. Our method capitalizes on the rich semantic content of audio to generate audio-assisted pseudo-labels, a new concept in the context of video TTA. Specifically, we propose an audio-to-video label mapping method by first employing pre-trained audio models to classify audio signals extracted from videos and then mapping the audio-based predictions to video label spaces through large language models, thereby establishing a connection between the audio categories and video labels. To effectively leverage the generated pseudo-labels, we present a flexible adaptation cycle that determines the optimal number of adaptation iterations for each sample, based on changes in loss and consistency across different views. This enables a customized adaptation process for each sample. Experimental results on two widely used datasets (UCF101-C and Kinetics-Sounds-C), as well as on two newly constructed audio-video TTA datasets (AVE-C and AVMIT-C) with various corruption types, demonstrate the superiority of our approach. Our method consistently improves adaptation performance across different video classification models and represents a significant step forward in integrating audio information into video TTA. Code: <https://github.com/keikeiqi/Audio-Assisted-TTA>.

**Index Terms**—Test-time adaptation, Video classification, Audio-assisted, Out-of-distribution generalization, Robustness

## I. INTRODUCTION

DEEP neural networks have achieved significant success in various video analysis tasks [1]–[4], but most methods assume that training and testing data come from the same distribution. This assumption often fails in real-world scenarios,

This work was supported by the National Natural Science Foundation of China (NSFC) (Grant Nos. 62202311, 62376099), Excellent Science and Technology Creative Talent Training Program of Shenzhen Municipality (Grant No. RCBS20221008093224017), Guangdong Basic and Applied Basic Research Foundation (Grant No. 2023A1515011512), Key Scientific Research Project of the Department of Education of Guangdong Province (Grant No. 2024ZDZX3012), and Natural Science Foundation of Guangdong Province (Grant No. 2024A1515010989). (Runhao Zeng and Qi Deng contributed equally to this work.) (Corresponding Authors: Shuaicheng Niu, Jian Chen)

Runhao Zeng, Xiping Hu and Victor C. M. Leung are with the Artificial Intelligence Research Institute, Shenzhen MSU-BIT University and Guangdong-Hong Kong-Macao Joint Laboratory for Emotional Intelligence and Pervasive Computing, Shenzhen, 518172, China. Qi Deng, Ronghao Zhang and Jian Chen are with School of Software Engineering, South China University of Technology, Guangzhou, 510000, China. Shuaicheng Niu is with College of Computing and Data Science, Nanyang Technological University, 639798, Singapore. E-mail: runhaozeng.cs@gmail.com; dengqi.kei@gmail.com; zhangronghao16@gmail.com; shuaicheng.niu@ntu.edu.sg; ellachen@scut.edu.cn; huxp@bit.edu.cn; vleung@ieee.org

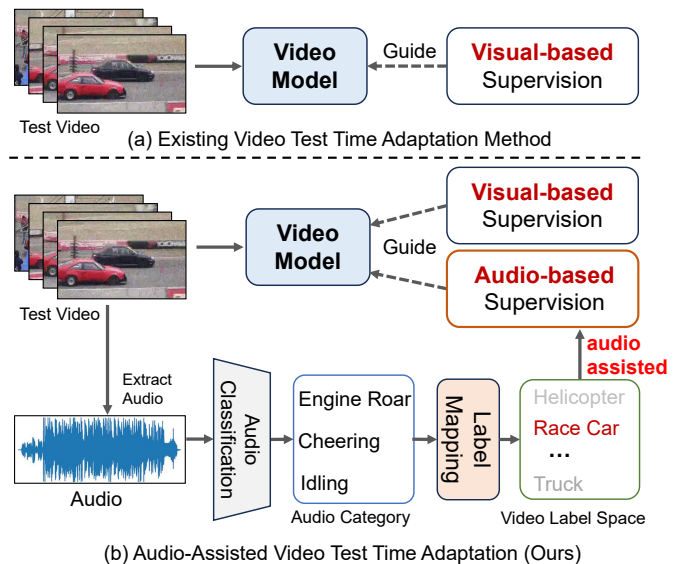


Fig. 1. Existing video test-time adaptation methods rely on visual supervision, overlooking the rich information inherent in audio. We propose a novel approach that involves extracting audio from videos and mapping the results of an open-source audio model to the video label space. This process generates audio-assisted pseudo labels, which significantly enhance TTA's performance.

where distribution shifts occur due to environmental factors such as lighting, geographic location, and camera models. As a result, there has been growing interest in test-time adaptation (TTA) methods, which aim to adapt to distribution shifts by leveraging test samples.

Although TTA methods have demonstrated effectiveness in image-based tasks [5]–[13], their performance in video tasks remains limited [14]. A key challenge in video TTA is that video models process a sequence of frames, and when visual corruption occurs, it disrupts both the sequential information and temporal coherence essential for accurate predictions, leading to a significant degradation in performance [15]. Recently, researchers have developed TTA methods tailored to video data [14]–[16]. As shown in Fig 1(a), these methods predominantly rely on visual information to obtain supervision (e.g., pseudo video label), neglecting the potential of audio as a supplementary modality.

In video data, audio and visual elements are often tightly synchronized and complementary. Human perception integrates both sensory modalities to better understand the environment. This becomes particularly relevant in real-world scenarios, where visual information may be degraded—due to adverse weather conditions, motion blur, or bandwidth

Case 1: Low visibility caused by severe fog



Case 2: Motion blur from camera shake



Case 3: Real-time video clarity compression in bandwidth-limited conditions



Fig. 2. Common scenarios of video disruption include challenging environmental conditions (Case 1), camera motion (Case 2), and transmission issues (Case 3). In these situations, the primary impact is on the visual content, while the audio remains relatively unaffected. Since video models tend to perform poorly when visual quality is degraded, combining both video and audio modalities offers a more robust solution.

limitations—while the audio stream remains relatively unaffected. For instance, as shown in Fig. 2, in conditions such as heavy fog or haze, visual sensors (e.g., cameras) may capture blurred or unrecognizable images, whereas the audio signal can still provide clear and informative content. Similarly, in fast-paced activities like parkour, motion blur can obscure visual details, yet the accompanying sounds (e.g., footsteps, environmental noises) remain informative. Additionally, in live video streaming, bandwidth constraints often result in compressed, low-quality video, while the audio stream may remain unaffected. These scenarios demonstrate that when visual data is compromised, audio can play a crucial role in enhancing the robustness of video classification models by providing complementary information.

However, integrating audio into TTA presents several challenges. In typical TTA settings, test data is unlabeled, making it impossible to directly train an audio classifier to predict video labels. A key challenge, therefore, is how to extract useful pseudo-labels from the audio to guide the adaptation of the video model. This issue is further complicated by the fact that audio and video label spaces are often mismatched, making it difficult to align audio-derived predictions with video action categories. For instance, as shown in Fig 1, when the audio contains predictions such as Engine Roar, Cheering and Idling, the corresponding video scene may involve actions like Race Car or Helicopter. To address this, a critical task is developing methods to map audio-derived pseudo-labels to the video label space without requiring additional training.

In this paper, we propose an audio-assisted approach for TTA in video models by leveraging the rich information embedded in audio, as illustrated in Fig 1. Our approach consists of two main components: audio-video label mapping and a flexible adaptation cycle. **First**, we utilize existing pre-trained audio models, such as AST [17], to obtain audio categories. However, the predicted audio categories are not directly aligned with the desired video categories due to differences in the label spaces of the two modalities. Fortunately, we observe that both audio and video labels are semantically

rich textual representations. Therefore, we propose a **audio-video label mapping** method based on large language models (LLMs), such as BERT [18] and GPT [19]. Specifically, we treat the predicted audio categories as text-related information relevant to the video and employ carefully designed prompting techniques. By leveraging the text comprehension abilities and knowledge inference capabilities of LLMs, we map these predicted audio categories to corresponding video labels. This enables the generation of pseudo video labels, which can serve as effective supervision for TTA.

**Second**, another challenge is the efficient utilization of the generated pseudo video labels. Our empirical findings indicate that performing TTA once per sample does not fully exploit the potential of audio-assisted pseudo labels. Performance can be further improved by repeating the adaptation for each sample. However, the optimal number of repetitions varies depending on the sample and the type of noise present. To address this, we propose a **flexible adaptation cycle** method, which designs adaptation conditions tailored to videos. This method uses the loss change between two consecutive adaptations and the consistency across different views of the same sample to determine the number of adaptations required. This allows for the adaptive selection of how many times pseudo video labels should be applied to each sample, ultimately achieving efficient audio-assisted TTA.

We construct two audio-video TTA datasets, AVE-C and AVMIT-C, by applying twelve common types of corruption to the videos. Additionally, we conduct experiments on video classification benchmarks, including UCF101-C and Kinetics-Sounds-C. Experimental results demonstrate that our method consistently improves adaptation performance across various backbone networks. Our main contributions are as follows:

- To our best knowledge, we are the first to explore integrating inherent audio from videos to boost the performance of a trained video model on out-of-distribution test samples via TTA. With the help of long-neglected audios, our proposed realistic but challenging paradigm can bring significant improvements over existing video TTA methods, e.g., 27% accuracy improvement over ViTTA on AVMIT-C dataset and TANet backbone.
- To effectively leverage audios, we propose a simple yet effective approach by utilizing Large Language Models to convert/align audio category space into any desired video label space to accommodate various datasets, without any additional training. To fully leverage audio-compensated labels, we devise a flexible adaptation cycle to dynamically determine the learning step of TTA for each test sample, further enhancing TTA performance.
- We achieve significant improvements over the state-of-the-art video TTA methods on not only the existing action recognition benchmarks (i.e., Kinetics-Sounds-C and UCF101-C) but also two novel audio-video TTA datasets (i.e., AVMIT-C and AVE-C) we develop. The efficacy and generality of our method have been tested across these four datasets and various backbones.

## II. RELATED WORK

### A. Test-Time Adaptation.

Recent advances in video models, particularly in human-centric action recognition [20]–[22], have achieved remarkable accuracy through specialized architectures and temporal modeling. However, these models often struggle with out-of-distribution (OOD) scenarios encountered in real-world settings, highlighting the need for effective TTA techniques. Test-time adaptation (TTA) tackles the adaptation to unknown distribution shifts at test time in an unsupervised manner. In recent years, it has garnered significant interest in the image domain [10], [11], [23]–[30]. One typical direction is to utilize a self-supervised auxiliary task to mitigate distribution shifts. For instance, TTT [12] adopted the self-supervised rotation prediction as an auxiliary task. TTT++ [13] proposed to use self-supervised contrastive learning. TENT [5] fine-tuned batch normalization’s affine parameters using an entropy penalty, whereas MEMO [6] adapted the network at test-time by minimizing the entropy of the marginal output distribution across augmentations. Although existing TTA methods achieve good results in image-based tasks, they do not perform as well in video-based tasks. Recently, TeCo [16] minimized the entropy of the prediction based on the global video content and fed local content to regularize the temporal coherence. AME [15] proposed to exploit motion cues to enhance the motion encoding capability of video models. ViTTA [14] aligned the testing statistics of certain layers with those derived from the training set, achieving the current best performance in video TTA. However, these methods largely depend on supervision derived from visual information, overlooking the rich data contained in audio. In this paper, we present a viable approach for utilizing audio in video TTA and empirically demonstrate that considering audio can significantly enhance the performance of TTA.

### B. Audio-Visual Learning for Video Classification.

Audio has been demonstrated to enhance action recognition performance beyond merely using visual modality alone [31]–[33]. One of the main components of the audio-visual learning algorithm is modality fusion, which can be categorized as early, mid, and late fusion [34]–[36]. Differing from these simple fusion strategies, the self-attention [37] operation of transformers provides a natural mechanism to aggregate audio-visual information [38]–[40]. Meanwhile, recent video understanding works like TAMT [41] demonstrated the effectiveness of multimodal fusion through timestamp-aligned visual frames and ASR transcripts for improved video summarization. [42], [43] conducted an analysis and research regarding the issue of modality imbalance in modal fusion. Recently, some works [44]–[46] considered that audio has less variance across domains to alleviate the domain shift in action recognition across scenes. Among the studies, the work most relevant to ours is [47]. They introduced an audio-infused recognizer to leverage domain-invariant cues inherent in the audio. However, their approach necessitates the pre-training of a model capable of taking audio input and producing corresponding video labels. This method is not feasible in our TTA setting, as we

lack the audio-label pairs for training. In our paper, we study a scenario more aligned with practical applications. Given any pre-trained video model, we propose a technique for extracting pseudo video labels from audio to facilitate TTA.

## III. PROPOSED METHOD

### A. Problem Statement

Consider  $P(v)$  as the distribution of a set of source training videos  $\{v_n\}_{n=1}^N$ , where each video  $v_n$  follows the distribution  $P(v)$ . A model, denoted as  $f_{\Theta}(\cdot)$  and parameterized by  $\Theta$ , is trained using labeled video samples  $\{v_n, y_n\}_{n=1}^N$ . The corresponding label for each video is  $y_n \in \mathcal{Y}_v$ , representing the label space. In an ideal scenario, the model  $f_{\Theta}(\cdot)$  should perform effectively on test samples that are drawn from the same distribution as the training set, namely  $v \sim P(v)$ . However, test samples often exhibit variations or corruptions not present in the training set, leading to out-of-distribution samples, denoted as  $v \sim U(v)$ , where  $U(v) \neq P(v)$ . This discrepancy typically results in substantial performance degradation.

To enhance the model’s generalization to out-of-distribution test samples, video test-time adaptation (TTA) [14] involves unsupervised learning at test time, utilizing only unlabeled test samples  $v$  to update the model  $f_{\Theta}(\cdot)$  in an online manner.

### B. General Scheme

We address the problem that existing video TTA methods primarily focus on visual information while neglecting the valuable audio cues present in videos. Audio, being less prone to visual noise, often contains important contextual information, such as object and scene cues, which can enhance the supervisory signals during testing. In this study, we propose leveraging the inherent audio signals in videos to improve the performance of video TTA.

Without loss of generality, given a video  $v$ , we forward it to a pre-trained video model to obtain classification prediction  $\hat{y}_v$ . To conduct TTA, we need a pseudo label  $\bar{y}$  and optimize the following loss function:

$$\mathcal{L}_{cls} = - \sum_{c=1}^C \bar{y}^c \log \hat{y}_v^c. \quad (1)$$

Unlike existing methods that derive  $\bar{y}$  from visual information, we propose using audio  $a$  extracted from videos to acquire reliable pseudo labels. To this end, we propose to exploit an open-source pre-trained audio classification model  $f_A$ , e.g., AST [17] to predict audio category  $\bar{y}_a$ , which are typically sound-related (e.g., crowd, water, fire, bus), differing completely from the video label space. Thus,  $\bar{y}_a$  cannot be directly used in Eqn.(1). To address this, we devise a **LLM-based Audio-to-Video Label Mapping** method to predict pseudo video label  $\bar{y}_v$  relying on the semantic relations between audio and video categories via

$$\bar{y}_v = f_L(P(f_A(a), \mathcal{Y}_v)), \quad (2)$$

where  $P$  is a prompt generator,  $\mathcal{Y}_v$  is the video label space, and  $f_L$  can be any large language model such as BERT [18],

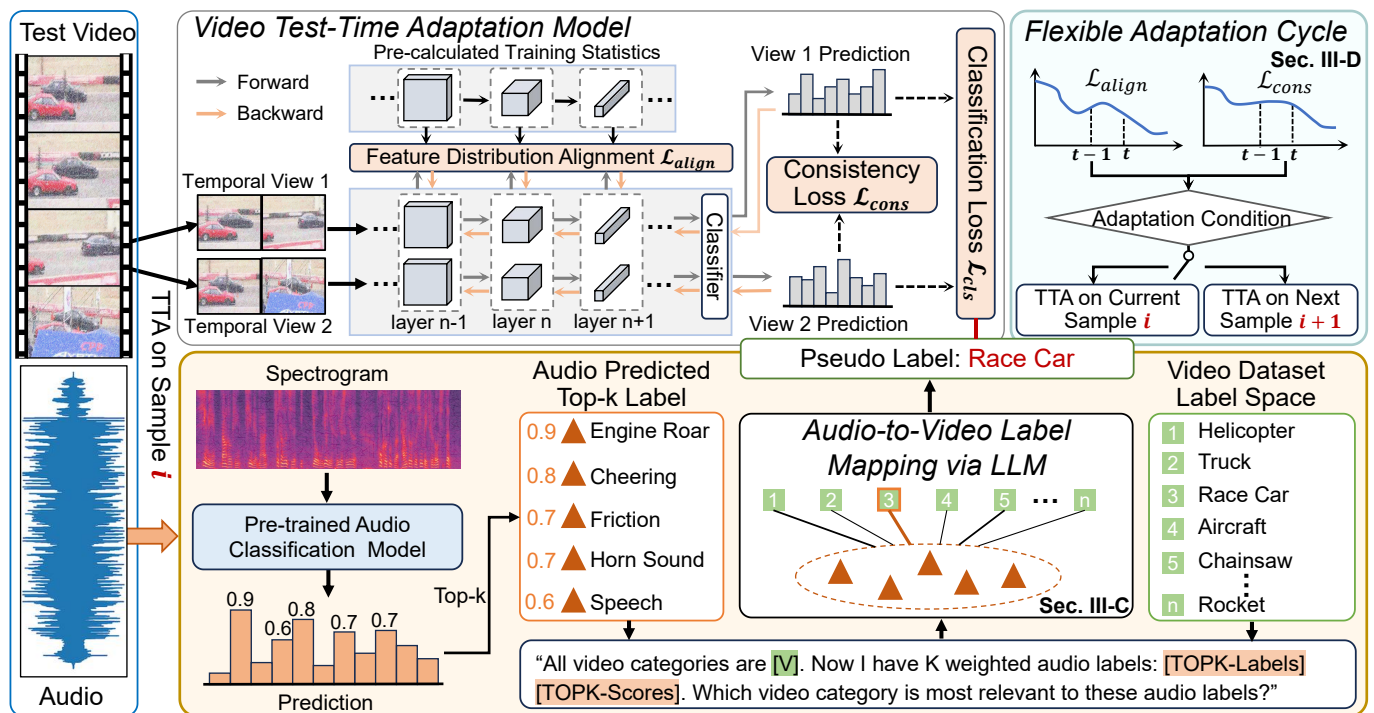


Fig. 3. Overall illustration of our proposed method. Given a paired video-audio test sample, we first extract audio labels using a pre-trained audio classification model and then align/map these audio labels with/to the video label space through a devised large language model (LLM) prompting technique. Next, we calculate the classification loss using these audio-assisted pseudo video labels for video TTA. Additionally, we propose a flexible adaptation cycle scheme to further boost adaptation performance by actively adjusting the learning iteration steps for each test sample based on a devised adaptation condition.

GPT [19]. Another challenge is how to use  $\bar{y}_v$  for TTA. Since the number of adaptations varies per sample, we propose an **Adaptive Audio-Visual Adaptation** method. In particular, we assess the consistency of predictions between the two views (w.r.t the same sample) and observe the change in loss between two adaptation steps, to select the number of adaptation steps for each sample. After each adaptation of an input test sample, we input the visual data of this sample into the updated video model for prediction. *In other words, the model, after undergoing adaptation through our method, can be deployed and make predictions under its original conditions (for example, using only visual data as input).* The schematic of our approach is shown in Fig 3. We organize the sections as follows:

- Sec. III-C details how to employ LLM to map audio labels to video labels, addressing the issue of label space mismatch between the audio and video labels.
- Sec. III-D introduces an additional model adaptation strategy that adaptively determines the number of adaptation steps for each sample, thereby enhancing the utilization of pseudo-video labels.

### C. Audio-to-Video Label Mapping via LLMs

The key challenge to obtain pseudo video label from audio input lies in the unknown labels of video and audio, compounded by the absence of an audio classifier corresponding to the video label space for direct prediction based on audio content. Training a dataset-specific audio classification model

with a label space identical to the video label space is resource-consuming and, more importantly, infeasible under the TTA setting.

To classify audio, we can leverage open-source pre-trained audio classification models  $f_A$  (e.g., AST [17]). However, the audio category obtained through this method cannot directly provide the corresponding video category. Therefore, we propose a pseudo label mapping method based on large language models (LLMs), utilizing LLMs  $f_L$  to infer the latent semantic association between audio categories and video labels, thereby deriving pseudo video labels. The key to exploiting LLMs lies in designing an efficient and reasonable prompt. Instead of simply inputting the audio prediction results and the labels contained in the corresponding video label space into the LLMs, we propose a template-based prompt generation module (PGM)  $f_P$ . Specifically, we select the top five categories with the highest scores in the predictions from  $f_A$ . Since the probability assigned to each category also reflects the confidence level, this is a crucial piece of information. We design a text prompt with five modules: Background, Task, Examples, Requirements, and Inputs, as follows: `#Human: "<Background Introduction><Task Description><Requirements><Examples><Inputs: video label space [V], audio predictions [TOPK-Labels] [TOPK-Scores]>."` `#Assistant: ,` where [TOPK-Labels] and [TOPK-Scores] denote the top-K predictions of the audio classification model and their predicted probability or confidence corresponding to each audio label, respectively. For a comprehensive view of the prompt, please refer to Fig. 7.

Overall, we input the video label space, the top five predictions of the audio model, and their probabilities into PGM and compute

$$\bar{y}_v = f_L(f_P(\mathcal{Y}_v, \bar{y}_a, \hat{p}_a)). \quad (3)$$

We sample frames from the same video for  $M$  times and forward them to the video model, lastly adapt the model by optimizing the following loss function

$$\mathcal{L}_{cls} = - \sum_{m=1}^M \bar{y}_v \log \hat{y}_v^m. \quad (4)$$

Note that we use only existing open-source models, obviating the need for additional training, which not only saves training costs but also aligns more closely with real-world application scenarios. Furthermore, this method has broad applicability and can be transferred to different datasets.

#### D. Adaptive Audio-Visual Adaptation

With the audio-assisted pseudo video label, one can utilize the loss calculated by Eqn. (4) to update the model. Then, proceed to the forward and backward adaptation of the next sample, a process we name single-step adaptation.

1) *Single-Step Audio-Visual Adaptation*: Besides acquiring supervision through audio as previously mentioned, we aim to further leverage supervision from the visual content. Specifically, we consider two types of loss, including cross-view consistency loss to exploit the relations between different views of the same sample and feature alignment loss to leverage the knowledge in the training set.

**Cross-view consistency loss.** We enforce consistency among the corresponding predictions of the  $M$  views. The learning target is obtained by averaging the class probabilities predicted by the video model for the input views, and the cross-view consistency loss is defined as

$$\mathcal{L}_{cons} = \sum_{m=1}^M \left| \hat{y}_v^m - \frac{1}{M} \sum_{j=1}^M \hat{y}_v^j \right|. \quad (5)$$

**Feature alignment loss.** We denote the feature maps from the  $l$ -th layer as  $g_l(v) \in \mathbb{R}^{c_l \times t_l \times h_l \times w_l}$  respectively,  $c_l$  is the number of channels in the  $l$ -th layer,  $t_l$  refers to the temporal dimension, and  $h_l$  and  $w_l$  represents the spatial dimensions. Hence, we compute the mean vectors of the  $l$ -th layer features by

$$\mu_l(v) = \mathbb{E}_{(i,j,z) \in V} [g_l(v)[:, i, j, z]], \quad (6)$$

where  $V = [1, t_l] \times [1, h_l] \times [1, w_l]$ . Based on the mean vectors, the variance vectors of the  $l$ -th layer features can be obtained by calculating

$$\sigma_l^2(v) = \mathbb{E}_{(i,j,z) \in V} [(g_l(v)[:, i, j, z] - \mu_l(v))^2]. \quad (7)$$

Our target is to align the testing statistics of selected layers to the statistics pre-calculated from the training data, by minimizing the following objective

$$\mathcal{L}_{align} = \sum_{l \in L} |\mu_l(T) - \hat{\mu}_l| + |\sigma_l^2(T) - \hat{\sigma}_l^2|, \quad (8)$$

---

#### Algorithm 1 Our Audio-Assisted Video TTA Method

---

**Require:** Test samples  $\{v_n\}_{n=1}^{N_t}$ , video label space  $\mathcal{Y}_v$ , pre-trained video model  $f_\Theta$  with parameters  $\Theta$ .

```

1: for  $i = 1 \dots N_t$  do
2:   // Get audio prediction
3:   Extract audio  $a_i$  from video  $v_i$ .
4:   Obtain top-K audio labels  $\bar{y}_a$  and probability  $\hat{p}_a$  using
   an open-source pre-trained audio model.
5:   // Pseudo Label Mapping via LLMs
6:   Get pseudo video label  $\bar{y}_v$  using LLMs via Eqn. (3).
7:   // Adaptive Audio-Visual Adaptation
8:   Initialize repetition step  $t = 0$ .
9:   while  $t < \tau$  do
10:    Calculate classification loss  $\mathcal{L}_{cls}$  relying on  $\bar{y}_v$  via
    Eqn. (4).
11:    Calculate consistency loss  $\mathcal{L}_{cons}$  via Eqn. (5).
12:    Compute mean and variance of the test data feature
    map layers via Eqn. (6) and (7).
13:    Calculate alignment loss  $\mathcal{L}_{align}$  via Eqn. (8).
14:    Update  $\Theta$  by minimizing the loss in Eqn. (9).
15:    // Adaptation condition
16:    Obtain  $R^t$  to determine whether to continue to adapt
    after the  $t$ -th repetition steps via Eqn. (10).
17:    Let  $t = t + 1$  if  $R^t = 1$  else break
18:  end while
19:  // Inference with visual data only
20:  Obtain video classification result:  $\hat{y}_i = f_\Theta(v_i)$ .
21: end for

```

---

where  $L$  is the set of layers to be aligned,  $|\cdot|$  denotes the vector  $l_1$  norm, recall that  $T$  denotes the test set,  $\hat{\mu}_l$  and  $\hat{\sigma}_l^2$  are pre-calculated training statistics. More details about  $\mathcal{L}_{cons}$  and  $\mathcal{L}_{align}$  please refer to [14]. The overall loss function of our audio-visual adaptation approach is

$$\mathcal{L} = \alpha \mathcal{L}_{cls} + \beta \mathcal{L}_{cons} + \mathcal{L}_{align}, \quad (9)$$

where  $\alpha$  and  $\beta$  are hyperparameters to trade off these losses. We set  $\alpha = \beta = 0.1$  in all the experiments and find that it works well across all of them.

2) *Multi-Step Adaptation via Flexible Adaptation Cycle*: We empirically found that adapting each sample only once may not yield good results (see Fig 5). Considering minor, even negligible, increases in time, significant gains can be achieved by repetitively adapting the same sample, thereby attaining better TTA results. However, simply allowing all samples to be adapted multiple times is impractical. We found that the number of adaptations required for each sample is dependent on the sample itself and the type of corruption it has undergone. While some samples may achieve excellent adaptation with very few rounds, others may necessitate a greater number. To address this, we propose a method named flexible adaptation cycle, which automatically selects the number of adaptation steps for each sample.

Our criteria for determining the adaptation cycle are based on the adaptation goal in Eqn. (9), with two primary considerations: the presence of a downward trend in loss and the consistency of predictions across different views. Our

TABLE I  
COMPARISON WITH STATE-OF-THE-ART TTA METHODS ON AVMIT-C AND AVE-C DATASET W.R.T. ACCURACY (%).

Dataset	Backbone	Methods	Corruptions												Avg.
			Gauss	Pepper	Salt	Shot	Contrast	Impulse	Rain	Zoom	Motion	Jpeg	Defocus	H265.abr	
AVMIT-C	TANet	Source	41.46	36.77	32.19	71.04	17.19	41.98	50.21	45.63	76.15	75.21	61.46	63.54	51.07
		BN-Adapt [48]	41.35	38.13	35.94	69.17	25.94	41.35	54.27	39.27	70.94	71.67	58.13	57.29	50.29
		TENT [5]	41.35	40.63	38.44	72.71	22.29	42.50	53.75	43.02	76.15	75.31	61.46	54.48	51.84
		SHOT [49]	43.44	41.25	39.69	71.56	26.98	44.90	58.54	44.17	75.94	74.06	62.08	62.29	53.74
		NORM [50]	49.79	42.50	41.15	72.40	29.27	48.85	74.79	55.62	72.29	71.56	56.56	50.42	55.43
		DeYO [51]	45.03	42.47	40.17	75.31	25.80	46.08	69.58	44.69	76.91	78.13	63.85	61.94	55.83
		ROID [52]	50.63	44.48	36.67	60.31	19.79	51.67	59.38	55.52	81.15	64.58	75.52	69.48	55.76
		VITTA [14]	52.71	49.58	38.65	77.19	37.08	52.71	70.21	55.63	76.56	77.08	65.42	64.27	59.76
		Ours	<b>72.40</b>	<b>63.85</b>	<b>65.73</b>	<b>84.06</b>	<b>63.65</b>	<b>71.88</b>	<b>80.94</b>	<b>72.81</b>	<b>83.75</b>	<b>86.56</b>	<b>78.85</b>	<b>72.92</b>	<b>74.78</b>
	TSM	Source	33.54	32.81	27.08	66.46	18.75	34.90	50.63	59.90	84.38	76.46	61.88	63.13	50.83
		BN-Adapt [48]	36.67	37.19	33.44	67.40	30.73	38.75	62.50	56.46	80.94	72.60	60.52	57.71	52.91
		TENT [5]	39.38	37.71	37.92	72.08	24.27	41.67	59.79	58.85	84.69	76.67	65.63	60.63	54.94
		SHOT [49]	40.83	38.23	39.37	68.75	35.52	42.81	65.21	58.23	82.40	74.17	63.44	61.46	55.87
		NORM [50]	40.00	42.50	34.12	64.79	25.63	49.27	67.40	49.27	64.48	64.17	55.73	45.52	50.24
		DeYO [51]	36.15	36.77	33.93	69.38	29.79	38.65	68.41	60.89	84.53	76.51	65.26	63.07	55.28
		ROID [52]	41.04	41.67	32.08	67.76	19.17	44.48	63.43	61.36	83.44	78.13	64.30	65.48	55.20
		VITTA [14]	45.73	42.40	33.13	71.77	25.42	46.15	59.90	60.00	84.48	76.77	65.63	63.33	56.23
		Ours	<b>52.60</b>	<b>45.83</b>	<b>39.38</b>	<b>75.31</b>	<b>43.65</b>	<b>56.77</b>	<b>71.15</b>	<b>62.60</b>	<b>85.31</b>	<b>78.54</b>	<b>67.81</b>	<b>66.98</b>	<b>62.16</b>
AVE-C	TANet	Source	35.82	35.32	23.38	60.20	20.40	35.57	56.97	42.29	68.41	48.26	50.75	51.24	44.05
		BN-Adapt [48]	27.36	32.59	21.39	59.20	13.68	27.36	61.69	42.79	65.42	47.26	49.75	44.53	41.09
		TENT [5]	24.13	30.85	18.41	60.70	19.40	22.89	61.44	43.28	67.66	48.76	55.47	46.52	41.63
		SHOT [49]	42.79	43.28	34.08	62.44	28.36	46.02	62.69	49.00	64.68	52.49	47.51	50.75	48.67
		NORM [50]	38.06	38.81	31.34	59.95	20.90	40.55	64.18	50.25	63.68	59.45	45.52	42.54	46.27
		DeYO [51]	39.55	35.57	25.87	64.93	20.65	41.29	64.93	43.53	67.91	53.23	53.48	51.00	46.83
		ROID [52]	40.42	38.93	24.88	72.14	24.38	40.30	66.79	49.75	68.78	53.98	57.59	57.71	49.64
		VITTA [14]	51.00	53.23	36.07	69.65	36.07	51.54	64.43	48.01	69.65	67.66	51.24	53.73	54.36
		Ours	<b>62.44</b>	<b>63.68</b>	<b>51.74</b>	<b>74.63</b>	<b>47.51</b>	<b>59.70</b>	<b>70.65</b>	<b>62.44</b>	<b>70.40</b>	<b>70.15</b>	<b>61.94</b>	<b>58.21</b>	<b>62.79</b>
	TSM	Source	26.37	31.84	19.15	59.20	12.69	26.12	51.24	44.28	65.67	48.26	48.26	50.25	40.28
		BN-Adapt [48]	29.10	34.33	24.38	56.22	17.41	29.60	60.20	47.26	67.16	47.02	53.23	46.77	42.72
		TENT [5]	27.86	32.34	23.13	59.45	19.40	27.11	60.45	49.01	66.67	48.76	55.22	46.27	42.97
		SHOT [49]	39.30	39.05	28.86	62.94	21.14	31.34	44.28	42.04	40.55	47.51	38.31	50.75	40.51
		NORM [50]	37.81	<b>48.26</b>	24.88	64.18	7.71	35.57	61.44	47.51	60.70	64.43	47.01	48.01	45.63
		DeYO [51]	30.22	34.45	24.73	59.58	23.22	32.09	60.35	49.50	66.24	51.74	52.92	50.75	44.65
		ROID [52]	29.10	43.53	20.90	70.40	11.69	30.60	59.20	52.74	66.92	62.94	49.00	57.96	44.65
		VITTA [14]	41.54	43.04	26.87	65.17	23.88	38.81	64.93	45.27	66.92	64.93	52.99	54.48	49.07
		Ours	<b>49.25</b>	48.01	<b>33.09</b>	<b>71.89</b>	<b>33.09</b>	<b>44.78</b>	<b>68.16</b>	<b>53.98</b>	<b>71.39</b>	<b>68.91</b>	<b>56.22</b>	<b>61.44</b>	<b>55.02</b>

underlying rationale, taking  $\mathcal{L}_{cons}$  as an illustration, is that for a given sample, if adaptation is executed consecutively twice and meets the criteria of  $\mathcal{L}_{cons}^{(t)} < \mathcal{L}_{cons}^{(t-1)}$ , this suggests a potential for further optimization, warranting continued adaptation using this sample. Regarding the two views of the same sample, if their predicted labels diverge  $\hat{y}_i^{(t)} \neq \hat{y}_j^{(t)}$ , we advocate for a new cycle of adaptation to this sample. To ensure efficiency, we also set a hyperparameter  $\tau$  that limits the maximum number of cycles. The criteria is defined as:

$$R^t = \mathbb{I}_{\{\mathcal{L}_{cons}^{(t)} < \mathcal{L}_{cons}^{(t-1)} \text{ or } \mathcal{L}_{align}^{(t)} < \mathcal{L}_{align}^{(t-1)} \text{ or } \hat{y}_i^{(t)} \neq \hat{y}_j^{(t)}\}}, \quad (10)$$

where  $\mathbb{I}_{\{\cdot\}}$  is an indicator function and  $R^t$  means whether to continue to adapt after the  $t$ -th cycle,  $i, j \in \{1, 2, \dots, M\}$ . In brief, if the current sample satisfies the conditions in Eqn. (10), it should undergo one more adaptation cycle. Otherwise, the adaptation should advance to the next sample. The algorithmic depiction of our adaptation method is shown in Algorithm 1.

#### IV. MAIN EXPERIMENTS

##### A. Dataset

In our paper, we conduct experiments on AVMIT-C (action recognition) and AVE-C (event/object localization), in which the audio and video are highly correlated, allowing us to assess the benefits of audio in video TTA effectively. We also conduct experiments on the UCF101 and Kinetics-Sounds datasets, two commonly used action recognition datasets. Despite the low audio accuracy in these two datasets, our method remains effective.

**Audiovisual Moments in Time (AVMIT)** [53] is a large-scale dataset of audiovisual action events. The dataset is collected from the Moments in Time dataset (MIT), comprising a total of 57,177 videos, each with a duration of 3 seconds. The test set consists of 960 videos, encompassing 16 common categories of human actions in daily life, with each category containing 60 videos.

**Audio-Visual Event (AVE)** [54] is a subset of AudioSet [55], that contains 4143 videos covering 28 event categories. The dataset includes audiovisual events from multiple domains, such as human activities, animal activities, music performances, and vehicle sounds. Each category contains at least 60 videos and at most 188 videos. The duration of the videos is at least 2 seconds, with approximately 66.4% of the videos being 10 seconds long. The entire dataset is divided into three parts: 3339 videos are used for the training set and 402 videos for the test set.

**UCF101** [56] is an action recognition dataset that provides 13,320 videos from 101 action categories. It is collected from YouTube and primarily includes five major categories of actions: interactions between people and objects, body movements, interactions between people, musical instrument performances, and sports activities. The official source provides three types of splits for dataset division. To follow ViTTA [14] and AME [15], we use the data of split 1, which consists of 9,537 and 3,783 videos for training and testing, respectively.

**Kinetics-Sounds** [33] is a subset of Kinetics dataset [57],

TABLE II  
COMPARISON WITH STATE-OF-THE-ART TTA METHODS ON UCF-C AND KINETICS-SOUNDS-C DATASET USING TANET W.R.T. ACCURACY (%). \*  
IMPLEMENT WITH OFFICIAL CODE.

Dataset	Methods	Corruptions												Avg.
		Gauss	Pepper	Salt	Shot	Contrast	Impulse	Rain	Zoom	Motion	Jpeg	Defocus	H265.abr	
UCF101-C	Source	17.92	23.66	7.85	72.48	76.04	17.16	37.51	54.51	83.40	62.68	81.44	81.58	51.35
	BN-Adapt [48]	40.81	37.70	26.27	83.79	73.49	41.84	88.19	81.32	60.68	87.08	49.80	80.61	62.63
	TENT [5]	19.35	26.57	8.83	77.19	79.38	18.64	40.68	58.61	86.12	67.22	84.00	83.45	54.17
	SHOT [49]	46.10	43.33	29.50	85.51	82.95	47.53	53.77	63.37	88.69	73.30	89.82	82.66	65.54
	NORM [50]	45.23	42.43	27.91	86.25	84.43	46.31	54.32	64.19	89.19	75.26	90.43	83.27	65.77
	ViTTA* [14]	69.78	64.18	44.68	<b>92.04</b>	87.64	71.53	68.35	80.53	91.59	86.97	92.62	84.53	77.87
	Ours	<b>71.66</b>	<b>66.46</b>	<b>47.40</b>	91.81	<b>88.07</b>	<b>72.72</b>	<b>71.34</b>	<b>81.63</b>	<b>91.62</b>	<b>87.30</b>	<b>92.68</b>	<b>84.31</b>	<b>78.92</b>
Kinetic-sound-C	Source	46.51	48.27	30.76	77.60	34.62	48.33	71.65	59.50	79.49	77.47	63.68	50.88	57.40
	BN-Adapt [48]	50.36	49.77	34.62	76.42	41.48	49.77	77.14	63.36	78.18	74.66	59.37	42.33	58.12
	TENT [5]	51.27	52.25	36.06	77.86	41.80	51.86	79.49	68.00	80.01	77.20	61.79	43.44	60.09
	SHOT [49]	55.52	54.28	38.34	78.25	45.85	55.26	79.88	69.89	<b>80.08</b>	77.47	63.49	45.00	61.94
	NORM [50]	51.34	51.86	36.12	77.60	41.28	51.40	78.84	67.21	79.69	76.81	61.53	43.37	59.75
	ViTTA* [14]	69.17	65.97	47.68	81.25	60.68	68.91	80.67	68.84	79.43	78.84	68.84	49.45	68.31
	Ours	<b>71.20</b>	<b>68.71</b>	<b>53.76</b>	<b>82.17</b>	<b>63.68</b>	<b>70.22</b>	<b>81.65</b>	<b>70.08</b>	79.29	<b>79.69</b>	<b>71.98</b>	<b>51.67</b>	<b>70.34</b>

TABLE III  
EFFECTIVENESS OF AUDIO INFORMATION FOR VIDEO TTA USING TANET W.R.T ACCURACY(%).

Dataset	Method	Corruptions												Avg.
		Gauss	Pepper	Salt	Shot	Contrast	Impulse	Rain	Zoom	Motion	Jpeg	Defocus	H265.abr	
AVMIT-C	w/o audio	52.71	49.58	38.65	77.19	36.77	51.88	71.15	56.35	75.10	77.19	65.42	60.73	59.39
	w/ audio	72.40	63.85	65.73	84.06	63.65	71.88	80.94	72.81	83.75	86.56	78.85	72.92	<b>74.78</b>
AVE-C	w/o audio	53.48	52.74	37.81	69.65	35.32	53.73	64.93	48.51	67.91	68.16	51.00	53.73	54.75
	w/ audio	62.44	63.68	51.74	74.63	47.51	59.70	70.65	62.44	70.40	70.15	61.94	58.21	<b>62.79</b>

which is a large-scale action recognition dataset sourced from YouTube. The Kinetics-Sounds dataset comprises 34 human action categories which have been chosen to be potentially manifested visually and aurally, with each category containing at least 400 videos. The dataset contains 15k training samples, 1.9k validation samples, and 1.9k test samples, and the duration of each video is approximately 10 seconds.

### B. Corruptions

We evaluate 12 types of corruption, which are introduced in [58], [59] and related to changes in light intensity, weather conditions, and noise that exist in practical applications. These 12 corruptions are: Gaussian noise, pepper noise, salt noise, shot noise, contrast, impulse noise, rain, zoom blur, motion blur, jpeg compression, defocus blur and H265.abr. Previous TTA methods [5], [14], [49], [50], including ViTTA, typically conduct experiments at severity level 5, as this represents the most challenging setting. To ensure a fair comparison with ViTTA, we also set the corruption severity level to 5.

### C. Model Architecture

We evaluate our approach on two different model architectures: TANet-R50 [60] and TSM-R50 [61], both of which are based on ResNet50 [62] for video classification. We use TANet as the default model unless otherwise specified.

### D. Implementation Details

We divide each video into 16 segments equally. A frame is randomly selected in the first segment, and 16 frames are sampled equidistantly. We set the batch size to 1 and perform online TTA. We use GPT-4 [63] as the default LLM.

**AVMIT-C dataset:** The learning rate for experiments using TANet as the backbone is set at  $5e-6$ , while for those using TSM as the backbone, it is set at  $1e-6$ . The maximum number of adaptation cycles,  $\tau$ , is set to 8 on both backbones.

**AVE-C dataset:** The learning rate for experiments with TANet as the backbone is set at  $1e-5$ , and for those with TSM as the backbone, it is maintained at  $1e-6$ .  $\tau$  is set to 8 and 4 respectively on two backbones, as the performance tends to stabilize when  $\tau$  exceeds 4 on TSM.

**UCF101-C and Kinetics-Sounds-C datasets:** We follow the learning rates provided by ViTTA for experiments. Using TANet as the backbone, we set the learning rates to  $5e-5$ , with  $\tau$  values of 3 and 2, respectively.

### E. Comparisons with State-of-the-Art

**Results on AVMIT-C and AVE-C.** We compare our proposed method with the state-of-the-art video TTA method (i.e., ViTTA [14]) and image-based TTA methods. We also implement a BN-Adapt baseline [48], which updates the running estimations of mean and variance statistics in batch normalization layers during adaptation. For fair comparisons, we use the same backbone feature extractors. The adaptation results on AVMIT-C and AVE-C are reported in Table I. It shows that image-based TTA methods achieve a slight improvement over those without adaptation. ViTTA is generally superior to those image-based approaches. However, there is still a noticeable gap when compared to our method. Our method consistently surpasses the aforementioned comparative methods across twelve different noise scenarios. This is due to our approach's ability to consider and utilize the latent audio information in videos, and its adaptive capacity to flexible adaptation cycle for each case, thereby achieving enhanced adaptive effects.

Video	Video model prediction before adaptation	Audio model prediction	Video model prediction after adaptation	Ground truth
	Violin, fiddle	Speech, Applause, ...	Male speech, man speaking	Male speech, man speaking
	Race car, auto racing	Vehicle, Aircraft, ...	Fixed-wing aircraft, airplane	Fixed-wing aircraft, airplane
	Bark	Animal, Goat, ...	Goat	Goat
	Train horn	Music, Banjo, ...	Banjo	Banjo

Fig. 4. Qualitative analysis of the results before and after adaptation using audio information.

**Results on UCF101-C and Kinetics-Sounds-C.** We present comparisons using the UCF101-C and Kinetics-Sounds-C datasets in Table II. On the Kinetics-Sounds-C dataset, our method improves the accuracy from 68.31% to 70.31%. For the UCF101 dataset, only 1944 samples (51.5%) contain audio, and even for those with audio, the audio-video correlation is relatively weak, as evidenced by the low pseudo-label accuracy of 9.67% on UCF101-C. Despite these challenges, our method still improves TTA performance from 77.87% to 78.92%, as shown in Table II. This improvement can primarily be attributed to the inclusion of two additional loss terms in Eqn. 9, which enables the use of both visual and audio cues for TTA.

## V. ABLATION STUDY

In this section, we conduct in-depth ablation experiments on four corruptions (unless otherwise specified), including Gauss, Pepper, Salt, and Shot, to understand the effectiveness of each proposed component.

### A. Does Audio-Assisted Supervision Help TTA?

Compared with existing TTA methods, our primary distinction lies in our utilization of audio information. For fair comparisons, we conduct experiments to contrast the scenarios with and without the use of audio (i.e., the  $L_{cls}$  in Eqn. (4)), while maintaining a flexible adaptation cycle in both cases. As illustrated in Table III, on the AVMIT-C and AVE-C datasets, the incorporation of audio consistently results in significant performance improvements under all 12 types of corruption, where enhancements reach approximately 15% and 8%, respectively. This underscores the effectiveness of our method stemming from the efficient use of audio. Our approach offers a novel perspective for enhancing TTA performance by leveraging multimodal information within videos.

**More qualitative analysis.** We further conduct a qualitative analysis on the AVE-C dataset to understand the effectiveness

of the proposed method in Figure 4. For example, in the first row, corruption significantly interferes with the visual information, leaving only a vague outline of the human body with no detailed motion features visible. In this scenario, the video model incorrectly predicts the action as “Violin, fiddle.” However, by leveraging the audio information from the video, we use the audio model to predict the categories “Speech” and “Applause”, which are then mapped to the video label “Male speech, man speaking” through the LLM. This process adapts the model, leading to a correct prediction by the video model. Other examples further demonstrate that audio information can provide reliable supervisory signals, especially when the video data is corrupted, thereby improving test-time adaptation performance.

### B. Do We Need Adaptation Cycle?

We aim to investigate whether it is feasible to utilize pseudo labels obtained by our method for multiple adaptations of the model. We incorporate a baseline, which involves setting  $\alpha = 0$  to remove the  $\mathcal{L}_{cls}$  term from Eqn. (9) (that is, not utilizing audio-assisted pseudo labels). This equals combining ViTTA [14] with multiple adaptations. Specifically, during the TTA process, each video sample from the online streaming input is tested after updating the model using Eqn. (9) for  $t \in \{1, 2, \dots, 7\}$  iterations. In each experiment, the number of adaptations per sample remains consistent.

The results in Fig 5 indicate that multiple adaptations are more effective than a single adaptation, suggesting the necessity of an adaptation cycle. We found that directly applying adaptation cycles to ViTTA without considering audio information is not effective. As the number of adaptations increases, the performance consistently decreases. Therefore, in this case, we only present the results of five cycles of ViTTA. This indicates that adaptation cycles need to be integrated with effective supervision. Our method offers a feasible approach for extracting supervisory information during TTA. Concurrently,

TABLE IV  
ABLATION OF FLEXIBLE ADAPTATION CYCLE ON AVE-C DATASET USING TANET W.R.T ACCURACY(%).

Method	Setting	Gauss	Pepper	Salt	Shot	Contrast	Impulse	Rain	Zoom	Motion	Jpeg	Defocus	H265.abr	Avg.
ViTTA	No cycle	51.00	53.23	36.07	69.65	36.07	51.54	64.43	48.01	69.65	67.66	51.24	53.73	54.36
	Fixed cycle	52.24	51.99	38.06	68.16	35.32	53.23	64.93	49.25	67.91	68.16	50.00	53.73	54.42
	Flexible cycle	53.48	52.74	37.81	69.65	35.32	53.73	64.93	48.51	67.91	68.16	51.00	53.73	<b>54.75</b>
Ours	No cycle	52.99	53.73	42.29	69.15	39.55	54.48	66.42	51.49	68.41	69.65	55.22	53.23	56.38
	Fixed cycle	57.21	59.95	49.25	69.90	43.78	61.19	69.40	61.94	71.14	67.91	59.70	60.20	60.97
	Flexible cycle	62.44	63.68	51.74	74.63	47.51	59.70	70.65	62.44	70.40	70.15	61.94	58.21	<b>62.79</b>

TABLE V  
ABLATION OF FLEXIBLE CYCLE CONDITIONS IN EQN. (10) USING TANET W.R.T AVERAGED ACCURACY ACROSS 12 TYPES OF CORRUPTION.

Dataset	$\mathcal{L}_{align}^{(t)} < \mathcal{L}_{align}^{(t-1)}$	$\mathcal{L}_{cons}^{(t)} < \mathcal{L}_{cons}^{(t-1)}$	$\hat{y}_i^{(t)} \neq \hat{y}_j^{(t)}$	Avg. Acc. (%)
AVMIT-C				71.91
	✓	✓		68.50
	✓		✓	72.07
		✓	✓	73.16
	✓	✓	✓	<b>74.78</b>
AVE-C				60.97
	✓	✓		59.10
	✓		✓	60.90
		✓	✓	61.82
	✓	✓	✓	<b>62.79</b>

TABLE VI  
RESULTS WITH PARTIALLY AVAILABLE PSEUDO LABELS USING TANET W.R.T AVERAGE ACCURACY(%) ACROSS 12 TYPES OF CORRUPTION.

Dataset	Source	ViTTA	Ratio of available pseudo label( $m\%$ )				
			20%	40%	60%	80%	100%
AVMIT-C	51.07	59.76	<b>60.12</b>	61.03	64.37	69.92	74.78
AVE-C	44.05	54.36	<b>55.06</b>	55.83	56.74	58.62	62.79

we also discovered that the optimal number of repetitions varies across different settings (different corruptions). This finding motivated us to design a flexible adaptation cycle.

### C. Does Flexible Adaptation Cycle Boost TTA?

To adaptively adjust the adaption steps for each sample, we propose a flexible adaptation cycle, wherein the criteria consider three conditions (Eqn. (10)):  $\mathcal{L}_{align}^{(t)} < \mathcal{L}_{align}^{(t-1)}$ ,  $\mathcal{L}_{cons}^{(t)} < \mathcal{L}_{cons}^{(t-1)}$ , and  $\hat{y}_i^{(t)} \neq \hat{y}_j^{(t)}$ . Our ablation experiments consider combinations of two conditions and the use of all three conditions and compare them with a scenario where no selection criteria are applied. For fair comparisons, in the absence of selection criteria, we also employ a strategy of multiple adaptation cycles and compare the best results obtained from the optimal number of cycles. The results in Table V indicate that using only the first two conditions as constraints leads to nearly unchanged or even slightly decreased accuracy. However, when condition 3, which assesses prediction consistency, is considered in combination with either condition 1 or 2, there is a significant performance improvement. This demonstrates the vital role of cross-view consistency in determining the adaptation cycle. When all conditions are combined, the results are optimal, suggesting that the flexible adaptation cycle strategy can effectively select

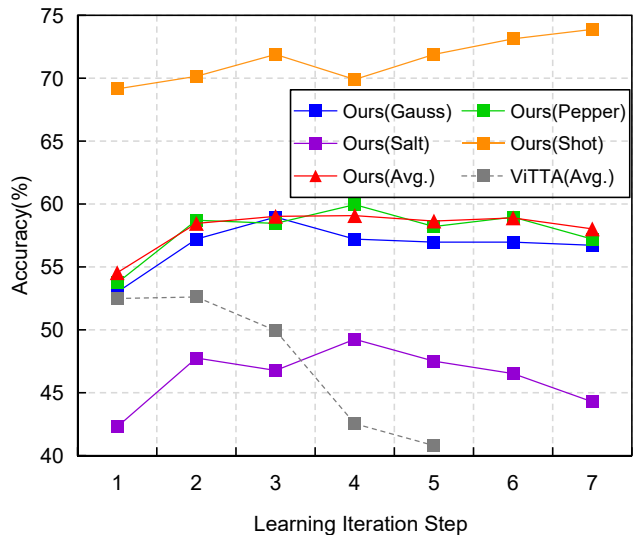


Fig. 5. Ablation on TTA's learning iteration steps (i.e., adaptation cycles) on TANet. Without using audio, ViTTA's accuracy drops significantly with more steps. The optimal step under different corruption types varies.

the number of sample repetitions, thereby achieving better TTA performance, as also verified in Table IV.

### D. When Pseudo Video Labels Are Not Readily Available?

In real scenarios, there may be instances where the audio corresponding to some videos is unobtainable, or there could be issues with network latency (e.g., when utilizing LLMs through API calls). These factors can ultimately lead to the inability to promptly acquire pseudo labels. Therefore, we design an experiment by keeping each video's pseudo label with a probability  $m\%$ , that is, simulating the situation where the entire dataset has only a probability of  $m\%$  that a pseudo video label can be obtained. From Table VI, even with only 20% of the pseudo video labels available in AVMIT-C and AVE-C, our method significantly outperforms ViTTA, demonstrating its practical applicability.

### E. Is our audio-assisted TTA method efficient?

We conduct runtime comparisons with TANet backbone using a single A800 GPU in Table VIII, revealing several key observations: **1)** Our approach operates in real-time, compatible with the practical video frame rate of 30 FPS. **2)** Our method is flexible, allowing for adjusting  $\tau$ , the maximum number of adaptation cycles, to accommodate varying

TABLE VII

RESULTS OF LABEL MAPPING ON AVMIT-C DATASET. BASED ON THE AUDIO LABELS AND THEIR PROBABILITY(SHOWN IN PARENTHESES) OBTAINED FROM THE AUDIO CLASSIFIER, LLM IS CAPABLE OF DELIVERING PLAUSIBLE PREDICTIONS.

Category 1	Category 2	Top-5 audio predictions			LLM prediction
		Category 3	Category 4	Category 5	
Dog(0.63)	Animal(0.61)	Domestic animals, pets(0.52)	Bark(0.44)	Bow-wow(0.44)	barking
Vehicle(0.60)	Lawn mower(0.20)	Propeller, airscrew(0.11)	Motorboat, speedboat(0.06)	Aircraft(0.06)	mowing
Music(0.47)	Drum(0.45)	Percussion(0.33)	Drum kit(0.25)	Drum roll(0.22)	drumming
Wood(0.95)	Rub(0.90)	Sawing(0.68)	Sanding(0.26)	Filing (rasp)(0.02)	sanding
Sizzle(0.19)	Frying (food)(0.14)	Spray(0.06)	Inside, small room(0.05)	Speech(0.04)	frying
Baby laughter(0.50)	Laughter(0.41)	Belly laugh(0.16)	Giggle(0.09)	Babbling(0.08)	giggling
Applause(0.56)	Rain on surface(0.19)	Raindrop(0.14)	Rain(0.10)	Sound effect(0.09)	raining
Vehicle(0.57)	Car(0.13)	Heavy engine(0.07)	Truck(0.06)	Car passing by(0.06)	mowing
Clicking(0.18)	Speech(0.06)	Stomach rumble(0.04)	Inside, small room(0.02)	Sound effect(0.02)	tapping
Boat, Water vehicle(0.15)	Gurgling(0.09)	Water(0.07)	Snort(0.06)	Rowboat, canoe, kayak(0.06)	diving
Animal(0.84)	Domestic animals, pets(0.79)	Dog(0.75)	Howl(0.73)	Canidae, dogs, wolves(0.33)	howling

TABLE VIII

COMPARISONS ON RUNTIME (SECONDS/VIDEO).  $\tau$ : THE MAXIMUM NUMBER OF ADAPTATION CYCLES FOR A SAMPLE,  $s$ : THE NUMBER OF DELAYED SAMPLES IN THE DELAYED UPDATE STRATEGY. WE REPORT THE AVERAGE ACCURACY UNDER FOUR TYPES OF CORRUPTION: GAUSS, PEPPER, SALT, AND SHOT.

AVMIT-C	Parallel Processing		Runtime	FPS	Accuracy(%)
	Video	Audio			
ViTTA	0.097s	N/A	0.097s	164.9	54.53
Ours( $\tau=1, s=0$ )	0.097s	0.260s	0.321s	49.8	59.22
Ours( $\tau=2, s=0$ )	0.161s	0.260s	0.385s	41.6	60.42
Ours( $\tau=4, s=0$ )	0.236s	0.260s	0.460s	34.8	66.40
Ours( $\tau=8, s=0$ )	0.301s	0.260s	0.525s	<b>30.5</b>	<b>71.51</b>
Ours( $\tau=1, s=1$ )	0.097s	0.260s	0.306s	52.3	59.38
Ours( $\tau=1, s=2$ )	0.097s	0.130s	0.194s	82.5	59.38
Ours( $\tau=1, s=4$ )	0.097s	0.065s	0.138s	115.9	58.91
Ours( $\tau=1, s=8$ )	0.097s	0.033s	0.110s	145.5	58.78
Ours( $\tau=1, s=16$ )	0.097s	0.016s	0.097s	<b>164.9</b>	<b>58.46</b>
Ours( $\tau=8, s=1$ )	0.301s	0.260s	0.510s	31.4	68.05
Ours( $\tau=8, s=2$ )	0.301s	0.130s	0.398s	40.2	67.32
Ours( $\tau=8, s=4$ )	0.301s	0.065s	0.342s	46.8	67.06
Ours( $\tau=8, s=8$ )	0.301s	0.033s	0.314s	51.0	63.18
Ours( $\tau=8, s=16$ )	0.301s	0.016s	0.301s	53.2	60.55

TABLE IX

RESULTS ON THE UCF101-C DATASET WITH OPTIONAL PROPOSED STRATEGIES USING TANET W.R.T. ACCURACY (%). THE RESULTS DEMONSTRATE THE EFFECTIVENESS OF THE PROPOSED STRATEGIES.

Methods	Corruptions				
	Gauss	Pepper	Salt	Shot	Avg.
ViTTA	71.37	64.55	45.84	91.44	68.30
Ours	71.66	66.46	47.40	91.81	69.33
Ours+ensemble	71.77	66.86	48.32	91.80	69.69
Ours+select	72.27	67.10	48.54	91.86	69.94
Ours+select+ensemble	72.40	67.47	49.20	91.86	<b>70.23</b>

FPS based on specific application requirements. To facilitate higher FPS, we propose a simple delayed update strategy. Specifically, given a continuous stream of test data, our model updates (incorporating TTA) only after processing a predefined number of samples, denoted as  $s$ . Within this period, we await the outcomes of pseudo video labels before applying model updates. Our approach consistently surpasses ViTTA across various  $s$  values. Notably, at  $\tau = 1$  and  $s = 16$ , our method significantly outperforms ViTTA (58.46% vs 54.53%) with the same 164.9 FPS.

### F. Analysis of LLM’s pseudo label predictions

Upon inputting this specified prompt into LLMs, we guide them to execute the process of label mapping. The results of label mapping on the AVMIT-C dataset are presented in Table VII. The first column of the table enumerates the top-5 audio labels along with their respective probabilities, marked by a colon separating the audio label and its probability. The second column demonstrates the most relevant video label chosen by LLMs from the video label space, based on the provided input. For instance, considering the first sample in the table, audio labels such as “Dog”, “Animal”, “Bark”, and others, each with a probability, are fed into LLMs. Utilizing these labels, LLMs deduce the video label to be “barking”, a conclusion that appears highly logical.

We analyze a subset of UCF101 (~1k samples) and identify three types of error in LLM’s predictions, as shown in Fig. 6: **1)** Different objects produce similar sounds. From the left example, the daf is also a type of drum. The audio produced is very similar, so it is difficult to distinguish it by audio alone. **2)** Mismatch between audio and vision. As shown in the middle example, the background music of the “IceDancing” is played by cello, there is no information that can reflect the ice dance in the audio. **3)** Similarity in ambient scene sounds. From the right example, the places corresponding to boxing and basketball are both sports halls. They both contain the sounds of people talking, cheering, and moving around. Therefore, it is difficult to distinguish specific actions when the ambient scene sound is similar. Despite these factors potentially leading to low accuracy of pseudo labels (e.g., 9.67% on UCF101), we still achieve better performance across 15 corruptions, i.e., 78.92% (ours) vs. 77.87% (ViTTA).

### G. Optional label filtering strategies

Consider a realistic situation, when the audio and video correlation is low, the pseudo labels may be unreliable. Therefore, based on our method, we additionally design two optional strategies and can choose whether to use or discard the pseudo label to obtain better performance. **1) Select strategy:** We assess the reliability of pseudo-labels by comparing them with video predictions. A pseudo-label is deemed trustworthy and therefore applicable if it ranks within the top- $k$  predictions for a given video. Otherwise, such a label will not be used in the



Fig. 6. Three cases of inaccurate LLM pseudo labels.

TABLE X  
COMPARISON OF THE IMPACT OF DIFFERENT LLMs ON AVMIT-C  
DATASET USING TANET W.R.T ACCURACY(%).

Method	LLM	Corruptions				
		Gauss	Pepper	Salt	Shot	Avg.
Source	-	41.46	36.77	32.19	71.04	45.37
ViTTA	-	52.71	49.58	38.65	77.19	54.53
Ours	GPT-4 [63] (Default)	72.40	63.85	65.73	84.06	71.51
	Claude-3-sonnet [64]	73.65	64.17	61.67	84.79	71.07
	Llama3 [65]	69.69	60.10	60.83	85.00	68.91
	Bing [66]	71.77	58.75	57.08	84.17	67.94

TTA process. **2) Ensemble strategy:** When the confidence of the predicted class (outputted by the video model) is below a threshold  $\theta$  and the pseudo label falls within the top- $k$  of video predictions, we adopt the pseudo label as the final prediction. Otherwise, we utilize the video prediction. As shown in Table IX, taking UCF101-C as an example with  $\theta$  set to 0.3 and  $k$  set to 10, the results show that each label filtering strategy brings further improvement. The best effect is achieved when both strategies are used at the same time.

#### H. More details about prompt design

Our prompt for pseudo label mapping consists of five modules: Background, Task, Examples, Requirements, and Inputs. We furnish contextual information about the task in the Background module, defining the specific task for Large Language Models (LLMs) to execute, and providing multiple illustrative examples. The Requirements module outlines a set of criteria, such as response formatting, to ensure uniformity in the outputs produced by LLMs. In the Inputs module, we supply LLMs with information such as the video label space, the top- $k$  audio labels of the samples, and their corresponding probabilities. This assists LLMs in accurately identifying the most relevant video label based on the content of the sample. The details of our prompt are illustrated in Fig. 7.

#### I. Impact of different LLMs

To assess the impact of different LLMs on the performance of our method, we employ various LLMs for label mapping. The experimental results are presented in Table X. Our findings show that all the tested LLMs effectively support our audio-assisted TTA method. Notably, the performance of the TTA method remained nearly identical when using GPT-4 [63] and Claude-3-Sonnet [64], suggesting that our approach is not dependent on a specific LLM.

#### J. Impact of different audio models

To evaluate the impact of different audio models on the performance of our method, we further validate our approach

#### Our proposed prompt for pseudo label mapping

##### <Background/Role Introduction>

Assuming you are Tom, you are highly skilled at analyzing audio and determining the type of sound.

On a video streaming website, there is a vast collection of videos, typically categorized with labels to aid users in searching and viewing. Videos fall into two modalities: visual (video) and auditory (audio). Now, I have isolated the audio from the videos and am attempting to classify videos solely based on their audio. The complete set of the video label space is provided in the Inputs module, with categories separated by '&' symbols. Each audio has been processed through an audio classification model, resulting in five most likely audio labels, each with corresponding weights.

##### <Task Description>

I will provide you with audio labels, and your task is to classify the audio into the appropriate video category. You should analyze the audio labels, with a focus on the ones with higher weights, and provide the corresponding video category, delivering the video category as the output result. The input format is as follows:

input:{Music:0.351, Vehicle:0.184, Lawn mower:0.118, Engine:0.081}

The format of input is similar to a dictionary in Python. Each input consists of multiple audio labels for a sound segment. The key, a concept in Python dictionary, represents the audio label, and the value represents the weight associated with that label. A higher weight indicates a higher likelihood of the presence of that sound in the audio.

##### <Requirements>

Since the audio labels are obtained from an audio model, in cases where there is only audio without visual information, the generated audio labels may not be entirely accurate. These labels might describe objects that can produce similar sounds. You should select the most likely video category. Please note that you need to select only one from the given video label space as the classification result.

Please note that videos on video-sharing websites may be manually processed, and may include background music or narration. These noises can significantly interfere with your ability to obtain useful audio information. When you cannot deduce an answer or when you encounter noise that prevents you from deducing the category, you should directly output {-1} as the answer.

Please based on the provided input, infer the corresponding video category. Simply output the results in the example format, and there is no need to restate the input or provide explanations.

##### <Examples>

input:{Scissors:0.218, Finger snapping:0.183, Computer keyboard:0.046, Sound effect:0.020, Typing:0.019}  
output:{tapping}

##### <Inputs>

video label space: {giggling & inflating & vacuuming & frying & sanding & tapping & drumming & howling & mowing & shredding & raining & barking & pouring & sneezing & diving & whistling}  
input:{Baby laughter:0.497, Laughter:0.408, Belly laugh:0.164, Giggle:0.087, Babbling:0.080}

Fig. 7. Our proposed prompt for pseudo label mapping.

by incorporating two other audio backbones: AuM [67] and BEATs [68]. As shown in Table XI, our audio-assisted TTA

TABLE XI  
PERFORMANCE OF DIFFERENT AUDIO MODELS ON AVE-C DATASET USING TANET W.R.T. ACCURACY (%).

Model	Corruptions												
	Gauss	Pepper	Salt	Shot	Contrast	Impulse	Rain	Zoom	Motion	Jpeg	Defocus	H265.abr	Avg.
Source	35.82	35.32	23.38	60.20	20.40	35.57	56.97	42.29	68.41	48.26	50.75	51.24	44.05
ViTTA	51.00	53.23	36.07	69.65	36.07	51.54	64.43	48.01	69.65	67.66	51.24	53.73	54.36
AST(Ours)	62.44	63.68	51.74	74.63	47.51	59.70	70.65	62.44	70.40	70.15	61.94	58.21	62.79
AuM	59.70	59.95	50.25	72.39	44.53	61.69	70.15	61.44	70.15	69.65	61.19	58.46	61.63
BEATs	60.95	61.94	53.23	72.64	51.00	61.19	71.64	61.19	71.14	69.90	61.69	61.69	63.18

TABLE XII  
PERFORMANCE ON THE AUDIO-VISUAL TIM MODEL ON AVE-C DATASET W.R.T. ACCURACY (%).

Method	Corruptions												
	Gauss	Pepper	Salt	Shot	Contrast	Impulse	Rain	Zoom	Motion	Jpeg	Defocus	H265.abr	Avg.
TIM [69]	72.71	70.92	65.45	78.78	51.59	72.64	75.10	63.18	75.97	77.99	73.51	67.31	70.43
TIM+Ours	<b>73.83</b>	<b>71.07</b>	<b>66.02</b>	<b>78.83</b>	<b>52.49</b>	<b>74.90</b>	<b>77.46</b>	<b>63.53</b>	<b>76.84</b>	<b>78.23</b>	<b>73.56</b>	<b>68.53</b>	<b>71.27</b>

method is compatible with these audio backbones, and it significantly improves video TTA performance compared to ViTTA. This demonstrates that our method is not restricted to a specific audio model, highlighting its generalizability.

#### K. Integration with audio-visual models

We combine our method with an audio-visual model, namely, TIM [69], which explicitly models the temporal interaction between audio and visual events in long videos and achieves SOTA performance in multimodal video recognition. Specifically, we train the model using clean training data, then test it under conditions of visual corruption and apply our method for test-time adaptation (TTA). As shown in Table XII, our method is compatible with the audio-visual model and improves its TTA performance when facing visual corruption. This combination highlights how our method can enhance the robustness of existing audio-visual models, particularly in challenging scenarios involving visual corruption, further supporting the practical value of our approach.

In real-world applications, audio information may not always be available. Our method ensures backward compatibility—if audio is unavailable during testing, the system reverts to the original visual-only performance. On the other hand, audio-visual models would fail in such situations, making our approach more robust in scenarios where audio is intermittently available.

#### L. Training statistics from different datasets

In the study detailed in Table XIII, we examine the efficacy of adapting a model to a test set by employing training statistics derived from another dataset. Our findings demonstrate that adaptation using training statistics from clean datasets consistently enhances model performance. This improvement is observed even when the training statistics are sourced from a dataset different from that of the test set. We observe that utilizing training statistics from either dataset for adaptation to the test set of the other incurs only a minimal performance decrement. This suggests robustness in model performance to variations in training statistics.

TABLE XIII  
MEAN TOP-1 CLASSIFICATION ACCURACY (%) OVER FOUR TYPES OF NOISE CORRUPTIONS, TO A TEST SET OF AVE-C WITH TRAIN STATISTICS FROM DIFFERENT DATASETS. WE PERFORM ADAPTATION ON TANET [60] AND TSM [61] IN COMBINATION OF DIFFERENT TRAIN AND TEST SETS ACROSS AVMIT AND AVE.

Test Set	Backbone	Methods	Source	Train Statistics	
				AVE	AVMIT
AVE-C	TANet	ViTTA	38.68	52.49	48.63
		Ours		<b>62.07</b>	<b>58.09</b>
	TSM	ViTTA	34.14	44.16	42.73
		Ours		<b>50.56</b>	<b>48.20</b>

## VI. CONCLUSION

Existing video TTA methods predominantly rely on visual information, neglecting the potential contribution of audio, which could offer valuable insights for enhancing TTA performance. In this work, we have introduced a novel audio-assisted video TTA framework that incorporates audio signals from videos to improve the generalization ability of video models. Specifically, we have proposed an LLM-based pseudo-label mapping method to address the challenge of aligning audio categories with the video label space, thereby facilitating audio-guided supervision. Additionally, we have introduced an adaptive strategy for determining the number of adaptation steps, which adjusts dynamically based on the data and the specific types of corruptions, optimizing the use of audio-assisted labels. Experimental results across four benchmark datasets have validated the effectiveness of our approach. Our findings provide a promising solution for integrating audio information in TTA contexts, enhancing the robustness of video models under diverse conditions.

## REFERENCES

- [1] Z. Wang, Q. She, and A. Smolic, "Action-net: Multipath excitation for action recognition," in *Proceedings of the IEEE Conference on Computer Vision and Pattern Recognition (CVPR)*, 2021, pp. 13 214–13 223.

- [2] W. Xiang, C. Li, B. Wang, X. Wei, X.-S. Hua, and L. Zhang, "Spatiotemporal self-attention modeling with temporal patch shift for action recognition," in *Proceedings of the European Conference on Computer Vision (ECCV)*, 2022, pp. 627–644.
- [3] J. Yang, X. Dong, L. Liu, C. Zhang, J. Shen, and D. Yu, "Recurring the transformer for video action recognition," in *Proceedings of the IEEE Conference on Computer Vision and Pattern Recognition (CVPR)*, 2022, pp. 14 063–14 073.
- [4] R. Zeng, W. Huang, M. Tan, Y. Rong, P. Zhao, J. Huang, and C. Gan, "Graph convolutional module for temporal action localization in videos," *IEEE Transactions on Pattern Analysis and Machine Intelligence*, vol. 44, no. 10, pp. 6209–6223, 2021.
- [5] D. Wang, E. Shelhamer, S. Liu, B. Olshausen, and T. Darrell, "Tent: Fully test-time adaptation by entropy minimization," in *Proceedings of the International Conference on Learning Representations (ICLR)*, 2021.
- [6] M. Zhang, S. Levine, and C. Finn, "Memo: Test time robustness via adaptation and augmentation," in *Advances in Neural Information Processing Systems (NeurIPS)*, 2022, pp. 38 629–38 642.
- [7] Y. Iwasawa and Y. Matsuo, "Test-time classifier adjustment module for model-agnostic domain generalization," in *Advances in Neural Information Processing Systems (NeurIPS)*, vol. 34, 2021, pp. 2427–2440.
- [8] M. J. Mirza, J. Micorek, H. Possegger, and H. Bischof, "The norm must go on: dynamic unsupervised domain adaptation by normalization," in *Proceedings of the IEEE Conference on Computer Vision and Pattern Recognition (CVPR)*, 2022, pp. 14 765–14 775.
- [9] M. Boudiaf, R. Mueller, I. Ben Ayed, and L. Bertinetto, "Parameter-free online test-time adaptation," in *Proceedings of the IEEE Conference on Computer Vision and Pattern Recognition (CVPR)*, 2022, pp. 8344–8353.
- [10] Y. Gandelsman, Y. Sun, X. Chen, and A. Efros, "Test-time training with masked autoencoders," in *Advances in Neural Information Processing Systems (NeurIPS)*, 2022, pp. 29 374–29 385.
- [11] S. Niu, J. Wu, Y. Zhang, Y. Chen, S. Zheng, P. Zhao, and M. Tan, "Efficient test-time model adaptation without forgetting," in *Proceedings of the International Conference on Machine Learning (ICML)*, 2022, pp. 16 888–16 905.
- [12] Y. Sun, X. Wang, Z. Liu, J. Miller, A. Efros, and M. Hardt, "Test-time training with self-supervision for generalization under distribution shifts," in *Proceedings of the International Conference on Machine Learning (ICML)*, 2020, pp. 9229–9248.
- [13] Y. Liu, P. Kothari, B. Van Delft, B. Bellot-Gurlet, T. Mordan, and A. Alahi, "Ttt++: When does self-supervised test-time training fail or thrive?" in *Advances in Neural Information Processing Systems (NeurIPS)*, 2021, pp. 21 808–21 820.
- [14] W. Lin, M. J. Mirza, M. Kozinski, H. Possegger, H. Kuehne, and H. Bischof, "Video test-time adaptation for action recognition," in *Proceedings of the IEEE Conference on Computer Vision and Pattern Recognition (CVPR)*, 2023, pp. 22 952–22 961.
- [15] R. Zeng, Q. Deng, H. Xu, S. Niu, and J. Chen, "Exploring motion cues for video test-time adaptation," in *Proceedings of the 31st ACM International Conference on Multimedia*, 2023, pp. 1840–1850.
- [16] C. Yi, S. Yang, Y. Wang, H. Li, Y. Tan, and A. C. Kot, "Temporal coherent test time optimization for robust video classification," in *Proceedings of the International Conference on Learning Representations (ICLR)*, 2023.
- [17] Y. Gong, Y.-A. Chung, and J. Glass, "Ast: Audio spectrogram transformer," in *Annual Conference of the International Speech Communication Association (INTERSPEECH)*, 2021, pp. 571–575.
- [18] J. D. M.-W. C. Kenton and L. K. Toutanova, "Bert: Pre-training of deep bidirectional transformers for language understanding," in *Proceedings of the North American Chapter of the Association for Computational Linguistics: Human Language Technologies (NAACL-HLT)*, 2019, pp. 4171–4186.
- [19] T. Brown, B. Mann, N. Ryder, M. Subbiah, J. D. Kaplan, P. Dhariwal, A. Neelakantan, P. Shyam, G. Sastry, A. Askell *et al.*, "Language models are few-shot learners," in *Advances in Neural Information Processing Systems (NeurIPS)*, 2020, pp. 1877–1901.
- [20] D. Guo, K. Li, B. Hu, Y. Zhang, and M. Wang, "Benchmarking micro-action recognition: Dataset, methods, and applications," *IEEE Transactions on Circuits and Systems for Video Technology*, vol. 34, no. 7, pp. 6238–6252, 2024.
- [21] K. Li, X. Peng, D. Guo, X. Yang, and M. Wang, "Repetitive action counting with hybrid temporal relation modeling," *IEEE Transactions on Multimedia*, 2025.
- [22] K. Li, D. Guo, G. Chen, C. Fan, J. Xu, Z. Wu, H. Fan, and M. Wang, "Prototypical calibrating ambiguous samples for micro-action recognition," *arXiv preprint arXiv:2412.14719*, 2024.
- [23] Y. Iwasawa and Y. Matsuo, "Test-time classifier adjustment module for model-agnostic domain generalization," in *Advances in Neural Information Processing Systems (NeurIPS)*, 2021, pp. 2427–2440.
- [24] Y. Su, X. Xu, and K. Jia, "Revisiting realistic test-time training: Sequential inference and adaptation by anchored clustering," in *Advances in Neural Information Processing Systems (NeurIPS)*, 2022, pp. 17 543–17 555.
- [25] Z. Nado, S. Padhy, D. Sculley, A. D'Amour, B. Lakshminarayanan, and J. Snoek, "Evaluating prediction-time batch normalization for robustness under covariate shift," *arXiv preprint arXiv:2006.10963*, 2020.
- [26] A. Khurana, S. Paul, P. Rai, S. Biswas, and G. Aggarwal, "Sita: Single image test-time adaptation," *arXiv preprint arXiv:2112.02355*, 2021.
- [27] M. Boudiaf, R. Mueller, I. Ben Ayed, and L. Bertinetto, "Parameter-free online test-time adaptation," in *Proceedings of the IEEE Conference on Computer Vision and Pattern Recognition (CVPR)*, 2022, pp. 8344–8353.
- [28] K. Chen, T. Gong, and L. Zhang, "Camera-aware recurrent learning and earth mover's test-time adaption for generalizable person re-identification," *IEEE Transactions on Circuits and Systems for Video Technology*, vol. 34, no. 1, pp. 357–370, 2023.
- [29] J. Liu, J. Xie, F. Zhou, and S. He, "Question type-aware debiasing for test-time visual question answering model adaptation," *IEEE Transactions on Circuits and Systems for Video Technology*, 2024.
- [30] Y. Wu, G. Chen, L. Ye, Y. Jia, Z. Liu, and Y. Wang, "Ttagaze: Self-supervised test-time adaptation for personalized gaze estimation," *IEEE Transactions on Circuits and Systems for Video Technology*, 2024.
- [31] W. Wang, D. Tran, and M. Feiszli, "What makes training multi-modal classification networks hard?" in *Proceedings of the IEEE Conference on Computer Vision and Pattern Recognition (CVPR)*, 2020, pp. 12 695–12 705.
- [32] H. Alwassel, D. Mahajan, B. Korbar, L. Torresani, B. Ghanem, and D. Tran, "Self-supervised learning by cross-modal audio-video clustering," in *Advances in Neural Information Processing Systems (NeurIPS)*, 2020, pp. 9758–9770.
- [33] R. Arandjelovic and A. Zisserman, "Look, listen and learn," in *Proceedings of the IEEE international conference on computer vision*, 2017, pp. 609–617.
- [34] E. Kazakos, A. Nagrani, A. Zisserman, and D. Damen, "Epic-fusion: Audio-visual temporal binding for egocentric action recognition," in *Proceedings of the IEEE International Conference on Computer Vision (ICCV)*, 2019, pp. 5492–5501.
- [35] C. Wang, H. Yang, and C. Meinel, "Exploring multimodal video representation for action recognition," in *Proceedings of International Joint Conference on Neural Networks (IJCNN)*, 2016.
- [36] C. Feichtenhofer, H. Fan, J. Malik, and K. He, "Slowfast networks for video recognition," in *Proceedings of the IEEE International Conference on Computer Vision (ICCV)*, 2019, pp. 6202–6211.
- [37] A. Vaswani, N. Shazeer, N. Parmar, J. Uszkoreit, L. Jones, A. N. Gomez, L. Kaiser, and I. Polosukhin, "Attention is all you need," in *Advances in Neural Information Processing Systems (NeurIPS)*, 2017, pp. 5998–6008.
- [38] V. Likhoshesterov, A. Arnab, K. Choromanski, M. Lucic, Y. Tay, and M. Dehghani, "Polyvit: Co-training vision transformers on images, videos and audio," *Transactions on Machine Learning Research*, vol. 2023, 2023.
- [39] A. Nagrani, S. Yang, A. Arnab, A. Jansen, C. Schmid, and C. Sun, "Attention bottlenecks for multimodal fusion," in *Advances in Neural Information Processing Systems (NeurIPS)*, 2021, pp. 14 200–14 213.
- [40] J. Chen and C. M. Ho, "Mm-vit: Multi-modal video transformer for compressed video action recognition," in *Proceedings of the IEEE Winter Conference on Applications of Computer Vision (WACV)*, 2022, pp. 1910–1921.
- [41] X. Shang, Z. Yuan, A. Wang, and C. Wang, "Multimodal video summarization via time-aware transformers," in *Proceedings of the 29th ACM International Conference on Multimedia*, 2021, pp. 1756–1765.
- [42] T. Chen, Z. Tan, T. Gong, Q. Chu, Y. Wu, B. Liu, N. Yu, L. Lu, and J. Ye, "Bootstrapping audio-visual video segmentation by strengthening audio cues," *IEEE Transactions on Circuits and Systems for Video Technology*, 2024.
- [43] J. Fu, J. Gao, B.-K. Bao, and C. Xu, "Multimodal imbalance-aware gradient modulation for weakly-supervised audio-visual video parsing," *IEEE Transactions on Circuits and Systems for Video Technology*, 2023.

- [44] M. Planamente, C. Plizzari, E. Alberti, and B. Caputo, "Cross-domain first person audio-visual action recognition through relative norm alignment," *arXiv preprint arXiv:2106.01689*, 2021.
- [45] —, "Domain generalization through audio-visual relative norm alignment in first person action recognition," in *Proceedings of the IEEE Winter Conference on Applications of Computer Vision (WACV)*, 2022, pp. 1807–1818.
- [46] L. Yang, Y. Huang, Y. Sugano, and Y. Sato, "Epic-kitchens-100 unsupervised domain adaptation challenge for action recognition 2021: Team m3em technical report," *arXiv preprint arXiv:2106.10026*, 2021.
- [47] Y. Zhang, H. Doughty, L. Shao, and C. G. Snoek, "Audio-adaptive activity recognition across video domains," in *Proceedings of the IEEE Conference on Computer Vision and Pattern Recognition (CVPR)*, 2022, pp. 13 791–13 800.
- [48] Z. Nado, S. Padhy, D. Sculley, A. D'Amour, B. Lakshminarayanan, and J. Snoek, "Evaluating prediction-time batch normalization for robustness under covariate shift," *arXiv preprint arXiv:2006.10963*, 2020.
- [49] J. Liang, D. Hu, and J. Feng, "Do we really need to access the source data? source hypothesis transfer for unsupervised domain adaptation," in *Proceedings of the International Conference on Machine Learning (ICML)*, 2020, pp. 6028–6039.
- [50] S. Schneider, E. Rusak, L. Eck, O. Bringmann, W. Brendel, and M. Bethge, "Improving robustness against common corruptions by covariate shift adaptation," in *Advances in Neural Information Processing Systems (NeurIPS)*, 2020, pp. 11 539–11 551.
- [51] J. Lee, D. Jung, S. Lee, J. Park, J. Shin, U. Hwang, and S. Yoon, "Entropy is not enough for test-time adaptation: From the perspective of disentangled factors," in *The Twelfth International Conference on Learning Representations, ICLR*, 2024.
- [52] R. A. Marsden, M. Döbler, and B. Yang, "Universal test-time adaptation through weight ensembling, diversity weighting, and prior correction," in *Proceedings of the IEEE/CVF Winter Conference on Applications of Computer Vision*, 2024, pp. 2555–2565.
- [53] M. Joannou, P. Rotshtein, and U. Noppeney, "Audiovisual moments in time: A large-scale annotated dataset of audiovisual actions," *arXiv preprint arXiv:2308.09685*, 2023.
- [54] Y. Tian, J. Shi, B. Li, Z. Duan, and C. Xu, "Audio-visual event localization in unconstrained videos," in *Proceedings of the European Conference on Computer Vision (ECCV)*, 2018, pp. 247–263.
- [55] J. F. Gemmeke, D. P. Ellis, D. Freedman, A. Jansen, W. Lawrence, R. C. Moore, M. Plakal, and M. Ritter, "Audio set: An ontology and human-labeled dataset for audio events," in *Proceedings of the IEEE Conference on Acoustics, Speech and Signal Processing (ICASSP)*, 2017, pp. 776–780.
- [56] K. Soomro, A. R. Zamir, and M. Shah, "Ucf101: A dataset of 101 human actions classes from videos in the wild," *arXiv preprint arXiv:1212.0402*, 2012.
- [57] W. Kay, J. Carreira, K. Simonyan, B. Zhang, C. Hillier, S. Vijayanarasimhan, F. Viola, T. Green, T. Back, P. Natsev *et al.*, "The kinetics human action video dataset," *arXiv preprint arXiv:1705.06950*, 2017.
- [58] M. C. Schiappa, N. Biyani, S. Vyas, H. Palangi, V. Vineet, and Y. Rawat, "Large-scale robustness analysis of video action recognition models," in *Proceedings of the IEEE Conference on Computer Vision and Pattern Recognition (CVPR)*, 2023, pp. 14 698–14 708.
- [59] C. Yi, S. Yang, H. Li, Y.-p. Tan, and A. Kot, "Benchmarking the robustness of spatial-temporal models against corruptions," in *Proceedings of the Neural Information Processing Systems Track on Datasets and Benchmarks*, 2021.
- [60] Z. Liu, L. Wang, W. Wu, C. Qian, and T. Lu, "Tam: Temporal adaptive module for video recognition," in *Proceedings of the IEEE International Conference on Computer Vision (ICCV)*, 2021, pp. 13 708–13 718.
- [61] J. Lin, C. Gan, and S. Han, "Tsm: Temporal shift module for efficient video understanding," in *Proceedings of the IEEE International Conference on Computer Vision (ICCV)*, 2020, pp. 7083–7093.
- [62] K. He, X. Zhang, S. Ren, and J. Sun, "Deep residual learning for image recognition," in *Proceedings of the IEEE Conference on Computer Vision and Pattern Recognition (CVPR)*, 2016, pp. 770–778.
- [63] J. Achiam, S. Adler, S. Agarwal, L. Ahmad, I. Akkaya, F. L. Aleman, D. Almeida, J. Altenschmidt, S. Altman, S. Anadkat *et al.*, "Gpt-4 technical report," *arXiv preprint arXiv:2303.08774*, 2023.
- [64] Anthropic, "The claude 3 model family: Opus, sonnet, haiku." [Online]. Available: <https://api.semanticscholar.org/CorpusID:268232499>
- [65] A. Grattafiori, A. Dubey, A. Jauhri, A. Pandey, A. Kadian, A. Al-Dahle, A. Letman, A. Mathur, A. Schelten, A. Vaughan *et al.*, "The llama 3 herd of models," *arXiv preprint arXiv:2407.21783*, 2024.
- [66] dice2o, "Binggpt: Desktop application of new bing's ai-powered chat," GitHub Repository, 2024. [Online]. Available: <https://github.com/dice2o/BingGPT>
- [67] M. H. Erol, A. Senocak, J. Feng, and J. S. Chung, "Audio mamba: Bidirectional state space model for audio representation learning," *IEEE Signal Processing Letters*, 2024.
- [68] S. Chen, Y. Wu, C. Wang, S. Liu, D. Tompkins, Z. Chen, and F. Wei, "Beats: Audio pre-training with acoustic tokenizers," in *International Conference on Machine Learning, ICML*, 2023, pp. 5178–5193.
- [69] J. Chalk, J. Huh, E. Kazakos, A. Zisserman, and D. Damen, "Tim: A time interval machine for audio-visual action recognition," in *Proceedings of the IEEE/CVF Conference on Computer Vision and Pattern Recognition*, 2024, pp. 18 153–18 163.